Fabrication and nonlinear optical properties of nanoparticle silver oxide films

Yi Chiu, U. Rambabu, Ming-Hong Hsu, Han-Ping D. Shieh, Chien-Yang Chen, and Hsi-Hsiang Lin

Citation: Journal of Applied Physics **94**, 1996 (2003); doi: 10.1063/1.1589178
View online: http://dx.doi.org/10.1063/1.1589178
View Table of Contents: http://scitation.aip.org/content/aip/journal/jap/94/3?ver=pdfcov
Published by the AIP Publishing

Fabrication and nonlinear optical properties of nanoparticle silver oxide films

Yi Chiu[a)]
Department of Electrical and Control Engineering, National Chiao Tung University, 1001 Ta Hsueh Road, Hsinchu 300, Taiwan, Republic of China

U. Rambabu,[b)] Ming-Hong Hsu, and Han-Ping D. Shieh
Institute of Electro-Optical Engineering, National Chiao Tung University, 1001 Ta Hsueh Road, Hsinchu 300, Taiwan, Republic of China

Chien-Yang Chen and Hsi-Hsiang Lin
MIRL, Industrial Technology Research Institute, 159 Chung Hsing Road, Section 4, Chutung, Hsinchu 310, Taiwan, Republic of China

(Received 3 February 2003; accepted 12 May 2003)

We report the fabrication of nanoparticle silver oxide thin films by rf magnetron sputtering and characterization of their nonlinear optical properties. The chemical decomposition and reversibility of AgO_x compounds were studied by thermogravimetric analysis, differential scanning calorimetry, and x-ray diffraction. Electron spectroscopy for chemical analysis measurements revealed a 0.5 eV negative binding energy shift from AgO to Ag_2O phase. The effect of particle plasmon resonance was confirmed by the absorption band shift with increased Ag_2O particle size. The measured third-order nonlinear susceptibility ($\chi^3 = 3.4 \times 10^{-7}$ esu) and response time (27 ps) of the Ag_2O nanoparticles makes it promising for applications in all-optical switching devices and optical data storage systems. © *2003 American Institute of Physics.* [DOI: 10.1063/1.1589178]

I. INTRODUCTION

Nonlinear optical and electronic properties of nanosized metal particles have drawn considerable attention because of their strong and size-dependent plasmon resonance absorption.[1] In a metal nanoparticle system such as gold and silver dispersed in a transparent matrix, an absorption peak due to surface plasmon resonance is usually observed in the visible spectral region. Metal nanoparticles are of special interest as nonlinear materials for optical switching and computing because of their relatively large third-order nonlinearity (χ^3) and ultrafast response time. The main attraction of optical switching is that it enables routing of optical data signals without the need for conversion to electrical signals, and therefore makes it independent of data rates and protocols. As an example, the response time of copper nanocrystals is as short as 0.7 ps in the weak excitation limit.[2] Such an ultrafast nonlinear response is interpreted in terms of generation and relaxation of hot electrons.[2,3] The third-order nonlinear susceptibility χ^3 of metal particles dispersed in glass can be enhanced to the order of 10^{-7} esu near the surface plasmon resonance frequency.[4,5]

High density data storage systems with more than a few tens of gigabytes are needed for high definition TV (HDTV) or digital movie recording. To meet these requirements, intense research work has been focused on magneto-optical and phase change recording media. However, in an optical recording system, the laser beam spot size is limited by diffraction depending on the laser wavelength (λ) and the numerical aperture (NA) of the objective lens. Several super-resolution techniques have been developed to overcome the diffraction limit. One such system, called super-resolution near field structure (Super-RENS), was first demonstrated by Tominaga *et al.* by using Sb (15 nm) as a mask layer.[6] Very recently, another Super-RENS mode called light scattering center Super-RENS (LSC-SuperRENS) was introduced with silver oxide (AgO_x) as the mask or switching layer to achieve its super-resolution near field effect.[7]

AgO_x is a thermodynamically unstable material. It decomposes into Ag_2O at 220 °C and to metallic Ag and O_2 at around 410 °C.[8–11] Electron spectroscopy for chemical analysis (ESCA) or x-ray photoelectron spectroscopy (XPS) has been used to investigate silver based compounds for their chemical states and crystal structures. Most of the studies on silver based systems indicated a negative shift of the binding energy (BE) of the Ag $3d$ electrons as the oxidation state was increased,[12–15] while other studies observed no BE shift with increased oxidation states.[16–18] The observed binding energy shifts were very small (0.1–0.8 eV), which sometimes complicated the spectral interpretation.[13]

The objective of this work is to fabricate nanoparticle silver oxide films and to investigate their chemical reversibility, phase transformation, and nonlinear optical properties towards its applications in optical switching and data storage.

II. EXPERIMENT

AgO_x thin films were deposited on Corning glass substrates by rf magnetron sputtering from a high-purity Ag

a)Author to whom correspondence should be addressed; electronic mail: yichiu@mail.nctu.edu.tw
b)On leave from Center for Materials for Electronics Technology (C-MET), IDA Phase-II, HCL, Cherlapally, Hyderabad 500051, India.

(99.995%) target with a reactive gas mixture of Ar and O_2 at 2 sccm flow rate, followed by an annealing process. The base pressure of the sputtering chamber was 1.6×10^{-7} Torr. As-deposited AgO_x thin films were black-gray in color. The sputtering rate of the AgO_x thin films was 0.87 nm/min with 50 W sputtering power. The sputtering parameters were optimized in order to obtain nanosized AgO_x particles with uniform surface roughness. X-ray diffraction (XRD) of as-deposited and annealed AgO_x samples was carried out in the range of $2\theta=20°-60°$. The oxidation state and chemical composition of the AgO_x thin films annealed under different conditions were studied by ESCA. Thermogravimetric analysis (TGA) was carried out for 6.265 mg of AgO_x powder from room temperature (30 °C) to 500 °C under N_2 atmosphere. Similarly, differential scanning calorimetry (DSC) was performed on 5.3 mg of as-deposited AgO_x powder from room temperature to 500 °C under N_2 atmosphere.

Optical absorption spectra were recorded for the AgO_x samples with different particle sizes by using a double beam UV-Vis spectrophotometer. The third-order nonlinear susceptibility of the nanoparticle AgO_x thin films was measured by the Z-scan technique.[19] The excitation conditions in the Z-scan experiments were: (1) laser wavelength $\lambda=400$ nm, (2) laser pulse width $t_{\text{pulse}}=68$ fs, (3) time interval between pulses $T=10.7$ ns, (4) focused spot radius at the sample $r_{\text{spot}}=32\ \mu$m, (5) average power at the sample $p=100$ mW, and (6) peak power $P_{\text{pulse}}=1.6\times10^4$ W. The response time of AgO_x thin films was measured using a pump–probe experiment, which was an extension of the Z-scan technique.[20] The pump beam was set a few picoseconds ahead of the probe beam by controlling the position of the delay stage. The response time can be derived from the plot of normalized transmittance versus delay time. The samples used in the Z scan and pump–probe experiments were 20-nm-thick AgO_x films deposited on 720-μm-thick Corning 1737F glass substrates.

III. RESULTS AND DISCUSSION

AFM images of AgO_x thin films prepared by various sputtering powers are shown in Fig. 1. As the sputtering power increased, the AgO_x atoms agglomerated to form larger islands. This may be due to AgO_x atoms gaining higher kinetic energy at higher sputtering power. Above a threshold value (between 75 and 100 W), the AgO_x atoms can easily move on the substrate surface and try to agglomerate with other AgO_x atoms to form islands. Since the objective is to fabricate nanosize and uniform thin films of AgO_x, the sputtering power should be lower than the threshold to prevent the formation of large AgO_x islands. Accordingly, the sputtering power was chosen as 50 W and $O_2/(Ar+O_2)$ as 50%. As-deposited AgO_x thin films were amorphous in nature. To convert them into crystalline form, the samples were annealed at 220 °C for various time periods to study the effect of annealing duration on the particle size. As shown in the AFM images in Fig. 2, the average particle size of the samples annealed at 220 °C for 0.5, 3, 5, and 10 min was about 47, 66, 84, and 87 nm, respectively. Similarly, in order to examine the effect of film thickness on AgO_x particle size, 5, 10, 20, and 30 nm thick AgO_x films were deposited on glass substrates as described above. As shown in the AFM images in Fig. 3, the average particle size of AgO_x increased with thickness. Therefore, the suitable AgO_x thickness for fabricating AgO_x nanoparticles is less than 10 nm so that the particles are well spread and below 100 nm in size.

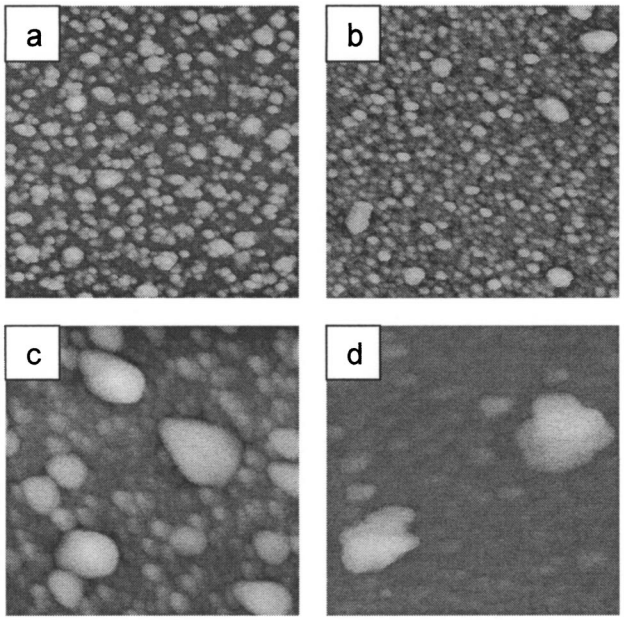

FIG. 1. AFM images ($1\times1\ \mu m^2$) of AgO_x thin films deposited with various sputtering powers: (a) 50, (b) 75, (c) 100, and (d) 125 W.

Thin silver films have the virtue of being oxidized by oxygen atoms but not by oxygen molecules. Their oxidation is temperature dependent. In order to observe the effect of

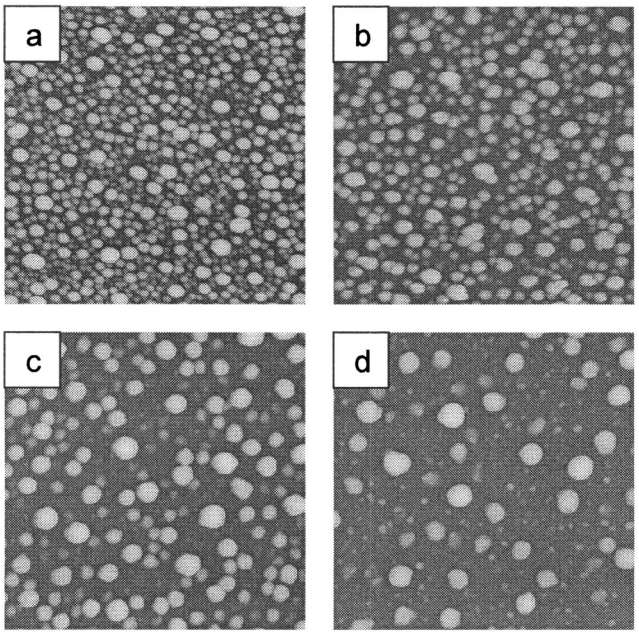

FIG. 2. AFM images ($1\times1\ \mu m^2$) of AgO_x thin films annealed at 220 °C for (a) 0.5, (b) 3, (c) 5, and (d) 10 min with average particle sizes of (a) 47, (b) 66, (c) 84, and (d) 87 nm, respectively.

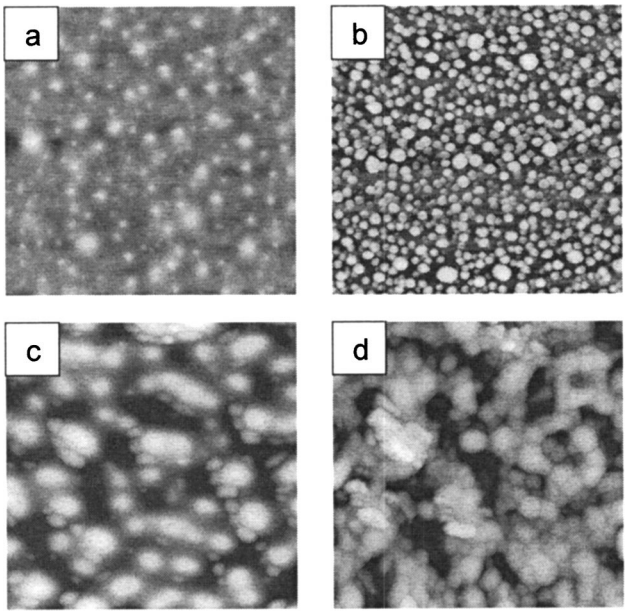

FIG. 3. AFM images ($1\times1\ \mu m^2$) of AgO_x thin films with (a) 5, (b) 10, (c) 20, and (d) 30 nm thickness. The average particle sizes are 35, 48, 114, and 124 nm, respectively.

annealing temperature on the phases of AgO_x, samples were annealed at various temperatures. Figure 4 shows the XRD spectra of samples annealed under various conditions: (a) as-deposited, (b) at 150 °C, (c) at 220 °C, and (d) at 420 °C for 5 min. It is observed that the as-deposited and 150 °C-annealed samples were in amorphous states. The reason that the sample annealed at 150 °C was still in amorphous state may be due to the short annealing duration or low annealing temperature. The samples annealed at 220 and 420 °C [Figs. 4(c) and 4(d)] had Ag_2O phase, a stable phase of silver oxides.

The chemical states of as-deposited and annealed AgO_x thin films were investigated by ESCA. The oxidation states of AgO_x can be identified from the shift of core-level binding energies in the ESCA spectrum. Gaarenstroom *et al.* did extensive work on the ESCA analysis of AgO and Ag_2O.[13,14] They observed a few tenths (0.4) of electron volts binding

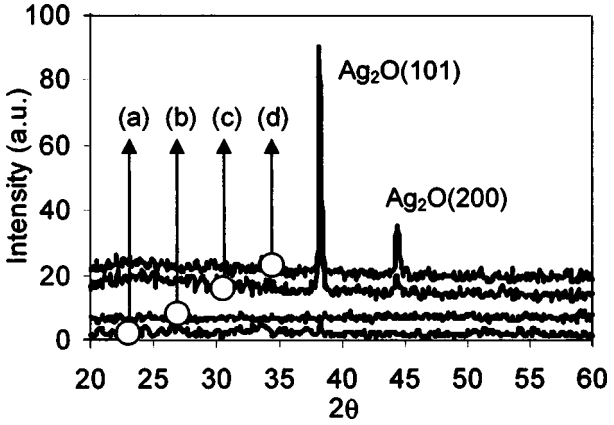

FIG. 4. XRD patterns of AgO_x thin films annealed at various temperatures: (a) as-deposited, (b) 150 °C, (c) 220 °C, and (d) 420 °C for 5 min.

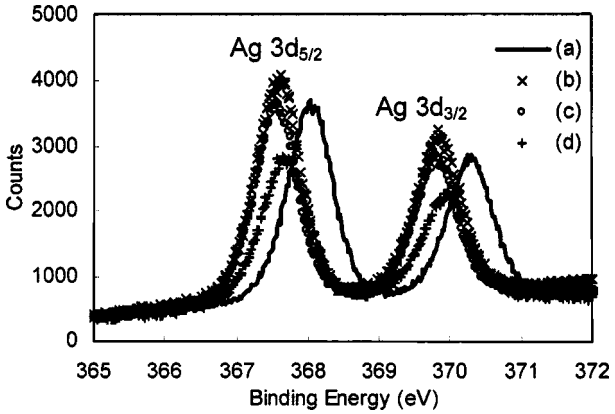

FIG. 5. ESCA spectra of Ag $3d_{3/2}$ and $3d_{5/2}$ peaks of AgO_x thin films annealed at various temperatures: (a) as-deposited, (b) 150 °C, (c) 220 °C, and (d) 420 °C for 30 min.

energy shift between AgO and Ag_2O phases. Figures 5(a)–5(d) represent the ESCA spectra of AgO_x thin films annealed at various temperatures for 30 min: (a) as-deposited, annealed at (b) 150 °C, (c) 220 °C, and (d) 420 °C. From the Ag $3d_{3/2}$ and $3d_{5/2}$ peaks in the ESCA spectra, it was noticed that the annealed samples [Figs. 5(b)–5(d)] had negative binding energy shift in the range of 0.4–0.5 eV compared to the as-deposited sample [Fig. 5(a)], which had a binding energy of 368.0 eV for the Ag $3d_{5/2}$ peak. Based on the XRD and ESCA results, it can be concluded that as-deposited AgO_x thin films are in silver peroxide (AgO) form and the annealed films are in the silver oxide (Ag_2O) phase.

TGA and DSC data of AgO_x are shown in Fig. 6. The thermal decomposition of AgO is a complicated process. AgO decomposes initially to form a solid solution of Ag_2O_3 and Ag_2O which then slowly decomposes into Ag_2O. The interpretation of such curves for determination of the AgO, Ag_2O, and Ag content of silver oxide samples was discussed by Parkhurt *et al.*[9]. From the TGA curve [Fig. 6(A)] of the AgO_x films, the main decomposition steps are: (1) an initial decomposition of AgO to Ag_2O (150–180 °C), (2) a slow continuing decomposition of AgO to Ag_2O (180–280 °C), and finally (3) a rapid decomposition of Ag_2O to metallic Ag

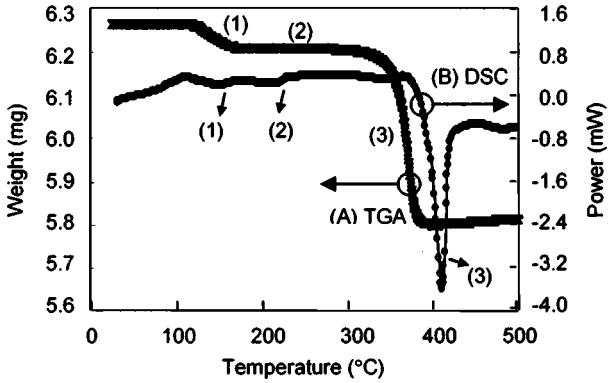

FIG. 6. (A) TGA curve of AgO_x powders (initial weight: 6.26 mg, end weight: 5.81 mg): (1) initial rapid decomposition of AgO to Ag_2O, (2) slow continuing decomposition of AgO to Ag_2O, and (3) rapid decomposition of Ag_2O to metallic Ag and O_2; (B) DSC curve of AgO_x powders with (1), (2), and (3) representing phase transitions as shown in TGA.

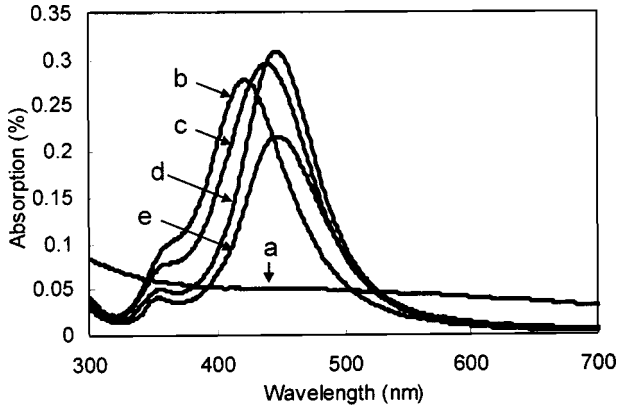

FIG. 7. Absorption spectra of deposited AgO_x thin films with various post-annealing conditions and particle sizes: (a) as deposited; annealed at 220 °C for (b) 0.5 min (47 nm), (c) 3 min (66 nm), (d) 5 min (84 nm), and (e) 10 min (87 nm).

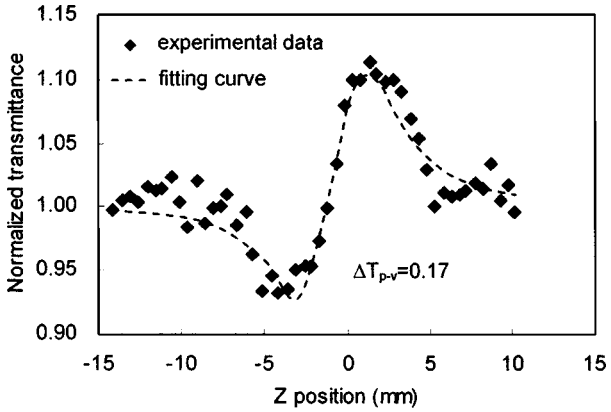

FIG. 8. Z-scan data with $S=0.4/S=1$ and laser wavelength of 400 nm.

and O_2 at about 385 °C. There is the possibility that the decomposition of Ag_2O may be initiated just prior to the completion of the AgO decomposition process near the very end of region (2).[9–11] The major decomposition chemical reactions of silver peroxide are:[8]

(i) $2AgO \rightarrow Ag_2O + 1/2O_2$

(ii) $Ag_2O \rightarrow 2Ag + 1/2O_2$.

Satisfactory agreement among the experimental results obtained by different authors about the true mechanism of Ag_2O decomposition remains unclear.[8] From the literature,[8–11] it is understood that the decomposition temperature peak positions of AgO_x may shift depending upon many factors such as the method of preparation, aging, contamination by CO_2 when exposed to environment, and the carrier gas and its pressure while measuring TGA and DSC. From the DSC curve [Fig. 6(B)], it is obvious that two weak endothermic peaks (1) and (2) at 150 and 220 °C represent the temperature of the phase transformations from AgO to Ag_2O as observed in TGA, respectively. The prominent endothermic peak (3) at 410 °C indicates the dissociation to metallic Ag and O_2. The temperature shift of peaks (3) in TGA and DSC of AgO_x was suspected owing to the contamination by CO_2 when exposed to the environment.[21] The thermal analyses showed a AgO_x decomposition reaction in the range of 385–410 °C. The XRD and ESCA patterns of AgO_x sample annealed at 420 °C showed the phase of Ag_2O. Based on the above analysis results, it is found that the AgO_x decomposition reaction is reversible. Therefore, it can be used as an optical switching layer in the phase-change volumetric optical recording systems.[22]

The absorption spectra of AgO_x thin films with different particle sizes and annealing conditions are shown in Fig. 7: (a) as-deposited; annealed at (b) 220 °C for 30 s with an average particle size of 47 nm, (c) 220 °C for 3 min with an average particle size of 66 nm, (d) 220 °C for 5 min with an average particle size of 84 nm, and (e) 220 °C for 10 min with an average particle size of 87 nm. The as-deposited AgO_x sample did not show any significant absorption band. For the annealed samples, the particle plasmon resonance absorption peaks were shifted from 420 to 450 nm with increased particle size. The peak absorption wavelength did not change in Figs. 7(d) and 7(e) due to nearly identical average particle sizes, but the peak absorption decreased with reduced particle density. By the Green's dyadic technique (GDT), Lamprecht demonstrated that the spectrally selective light absorption and scattering peaks shift to longer wavelength with increased gold nanoparticle size.[23] Our present absorption results are in agreement with the fact that the position of the particle plasmon resonance wavelength is mainly determined by the particle size and the peak absorption increases with increased particle density due to the increased volume of the particles.[23]

The Z-scan technique was used to characterize the nonlinear optical properties of AgO_x nanoparticles. A femtosecond frequency-doubled and mode-locked Ti-sapphire laser operating at 93.3 MHz was used as the light source. The laser pulse width was 68 fs and the frequency-doubled center wavelength was 400 nm. The source laser beam was separated into two beams by a beam splitter. One was detected as the reference irradiance I_1 by a photodetector D_1. The other was focused onto the sample with a lens and detected through an aperture S as the transmitted irradiance I_2 by another photodetector D_2. The normalized transmittance (I_2/I_1) was measured for various sample positions. The nonlinear refractive effect in AgO_x nanoparticles at 400 nm can be observed by dividing the normalized transmittance for a partially closed aperture $(S=0.4)$ by that for an open aperture $(S=1)$. As shown in Fig. 8, the difference between the peak and valley of the normalized transmittance (ΔT_{p-v}) was measured as 0.17. If the index change due to the optical Kerr effect is expressed as $\Delta n = \gamma I$, γ can be calculated as 3×10^{-13} m^2/W, which corresponds to a third-order nonlinear susceptibility, χ^3, of 3.4×10^{-7} esu for nanoparticle AgO_x.[19,24] In the calculation of the nonlinear refractive index γ, it was assumed that all the measured index change was due to the AgO_x film. Since the nonlinear refractive index of glass is in the range of 10^{-19}–10^{-20} m^2/W, the index change introduced by the glass substrate is about 1% of that by the AgO_x film even though the substrate is much thicker than the film. Therefore, the validness of the approximation can be justified. The measured nonlinearity of AgO_x is as high as that reported for the metal nanoparticles.[4,5,25] It

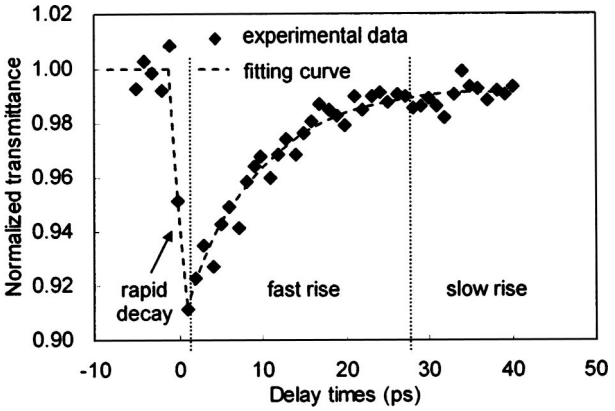

FIG. 9. Normalized transmittance at the laser wavelength of 400 nm vs probe delay.

should be noted that the metal nanoparticles in previous experiments were mostly dispersed in glass matrix with concentrations ranging from 10^{-4} to 10^{-1}. In AgO_x films, however, the atomic silver percentage is between 50% and 66%. Such a high silver percentage may account for the high nonlinearity for a nonmetallic material such as AgO_x.

In the pump–probe experiment, the probe beam was first set a few picoseconds behind the pump beam. A time-delay stage was then moved by a computer so that the pump beam gradually went ahead the probe beam. The pump beam would excite the sample before the probe beam arrived at the sample. Therefore, the probe signal could reflect the nonlinear interaction of the sample with the probe beam. The response time of an AgO_x thin film of average particle size of 47 nm was measured from the probe signal versus time delay curve as shown in Fig. 9. According to the literature,[23,25,26] the normalized transmittance curve can be divided into three regions: (1) rapid decay, (2) fast rise, and (3) slow rise regions. A rapid decay of the transmittance within the first picoseconds after excitation can be clearly observed. This is a result of heating the electrons by the high excitation of the pulse. The time constant of the rapid decay (<1 ps) corresponds to the thermalization time of electron-hole pairs excited by the energy of the decaying particle plasmon. The subsequent return of the heated electron gas to the equilibrium value is characterized by a two-component rise: the fast rise component with a time constant of about 27 ps corresponds to electron–phonon coupling in the AgO_x nanoparticles, whereas the second slow rise component with a time constant of more than 100 ps (not shown in Fig. 9) corresponds to heat transfer from the AgO_x nanoparticles to the glass substrate. By electron–phonon coupling, the hot electrons transfer energy to the crystal lattice and cool down on a picosecond time scale. The time constants of the rapid decay and the slow rise components of AgO_x nanoparticles are similar to those of pure Ag nanoparticles, whereas the time constant of fast rise component of AgO_x nanoparticles (27 ps) is longer than that of Ag (1.3 ps).[25] This may be due to the effect of oxygen atoms which can affect the electron–phonon coupling process and thus increase the time constant of the energy transfer between hot electrons and the crystal lattice.

IV. CONCLUSION

Material properties of deposited AgO_x nanoparticles were investigated. The particle plasmon resonance wavelength was shifted from 420 to 450 nm with increased Ag_2O particle size. The reversible nature of the decomposition reaction of Ag_2O was confirmed by TGA, DSC, XRD, and ESCA. From Z-scan and pump–probe experiments, the third-order nonlinear susceptibility (χ^3) and the response time of the deposited Ag_2O nanoparticles were measured as 3.4×10^{-7} esu and 27 ps, respectively. The nonlinearity is similar to that in the metal nanoparticle system. The high silver percentage in the AgO_x films may be used to prepare high-concentration metal silver nanoparticles to further enhance the nonlinearity. For all-optical switching applications, the nonlinearity and response time are comparable to other potential candidate materials such as semiconductor, organic materials, and metal nanoparticles. In optical storage systems, the standard channel bit rate for DVD is about 30 Mbps. The measured response time is therefore well suited for application of AgO_x as the switching or masking layer.

ACKNOWLEDGMENTS

This work was partially supported by MIRL/ITRI and by the Ministry of Education of the Republic of China under the Academic Center of Excellence in ''Photonics Science and Technology for Tera Era'' with Contract No. 89-E-FA06-1-4.

[1] U. Kreibig and M. Vollmer, *Optical Properties of Metal Clusters* (Springer, Berlin, 1995).
[2] T. Tokizaki, A. Nakamura, S. Kaneko, K. Uchida, S. Omi, H. Tanji, and Y. Asahara, Appl. Phys. Lett. **65**, 941 (1994).
[3] Y. Hamanaka, A. Nakamura, S. Omi, N. Del Fatti, F. Vallee, and C. Flytzanis, Appl. Phys. Lett. **75**, 1712 (1999).
[4] F. Hache, D. Ricard, C. Flytzanis, and U. Kreibig, Appl. Phys. A: Solids Surf. **47**, 347 (1988).
[5] K. Uchida, S. Kaneko, S. Omi, C. Hata, H. Tanji, A. Asahara, A. J. Ikushima, T. Tokizaki, and A. Nakamura, J. Opt. Soc. Am. B **11**, 1236 (1994).
[6] J. Tominaga, T. Nakano, and N. Atoda, Appl. Phys. Lett. **73**, 2078 (1998).
[7] J. Tominaga, J. Kim, H. Fuji, D. Buchel, T. Kikukawa, L. Men, H. Fukuda, A. Sato, T. Nakano, A. Tachibana, Y. Yamakawa, M. Kumagai, T. Kukaya, and N. Atoda, Jpn. J. Appl. Phys., Part 1 **40**, 1831 (2001).
[8] B. V. L'vov, Thermochim. Acta **333**, 13 (1999).
[9] W. A. Parkhurst, S. Dallek, and B. F. Larrick, J. Electrochem. Soc. **131**, 1739 (1984).
[10] S. Dallek, W. A. West, and B. F. Larrick, J. Electrochem. Soc. **133**, 2451 (1986).
[11] S. Dallek, W. A. Parkhurst, and B. F. Larrick, Thermochim. Acta **78**, 333 (1984).
[12] G. Schon, Acta. Chem. Scand. **27**, 2623 (1973).
[13] S. J. Hammond, S. W. Gaarenstroom, and N. Winograd, Anal. Chem. **47**, 2193 (1975).
[14] S. W. Gaarenstroom and N. Winograd, J. Chem. Phys. **67**, 3500 (1977).
[15] V. K. Kaushik, J. Electron Spectrosc. Relat. Phenom. **56**, 273 (1991).
[16] M. Romand, M. Roubin, and J. P. Deloume, J. Electron Spectrosc. Relat. Phenom. **13**, 229 (1978).
[17] R. Holm and S. J. Storp, J. Electron Spectrosc. Relat. Phenom. **8**, 459 (1976).
[18] C. Rehren, M. Muhler, X. Bao, R. Schlogl, and G. Ertl, Z. Phys. Chem. **174**, 11 (1991).
[19] M. Sheik-Bahae, A. A. Said, T.-H. Wei, D. J. Hagan, and E. W. van Stryland, IEEE J. Quantum Electron. **QE-26**, 760 (1990).

[20] G. L. Eesley, Phys. Rev. Lett. **51**, 2140 (1983).
[21] G. D. Nagy, J. B. Vergette, and J. P. Connolly, Can. J. Chem. **49**, 3986 (1971).
[22] F. S. Wu and H. P. D. Shieh, Jpn. J. Appl. Phys., Part 1 **41**, 1683 (2002).
[23] B. Lamprecht, Ph.D thesis, Institute for Experimental Physics, Karl-Franzens University of Graz, Australia, 2000.
[24] R. W. Boyd, *Nonlinear Optics* (Academic, New York, 1992).
[25] H. Inouye, K. Tanaka, I. Tanahashi, T. Hattori, and H. Nakatsuka, Jpn. J. Appl. Phys., Part 1 **39**, 5132 (2000).
[26] M. Perner, P. Bost, U. Lemmer, G. von Plessen, J. Feldmann, U. Becker, M. Mennig, M. Schmitt, and H. Schmidt, Phys. Rev. Lett. **78**, 2192 (1997).